



Predicting soil organic carbon stocks under future land use and climate change conditions in Northeast China

Shuai Wang^{a,b,c}, Xingyu Zhang^a, Kabindra Adhikari^d, Bol Roland^{c,f}, Qianlai Zhuang^e, Zicheng Wang^a, Di Shi^a, Xinxin Jin^{a,*}, Fengkui Qian^{a,*}

^a College of Land and Environment, Shenyang Agricultural University, Shenyang, Liaoning Province 110866, China

^b Key Laboratory of Ecosystem Network Observation and Modeling, Institute of Geographic Sciences and Natural Resources Research, CAS, Beijing 100101, China

^c Institute of Bio- and Geosciences, Agrosphere (IBG-3), Forschungszentrum Jülich GmbH, Wilhelm-Johnen-Straße, 52428 Jülich, Germany

^d USDA-ARS, Grassland, Soil and Water Research Laboratory, Temple, TX 76502, USA

^e Department of Earth, Atmospheric, and Planetary Sciences, Purdue University, West Lafayette, IN 47907, USA

^f School of Natural Sciences, Environment Centre Wales, Bangor University, Bangor LL57 2UW, UK

ARTICLE INFO

Keywords:

Carbon sequestration
Digital soil mapping
Future climate
Future land use

ABSTRACT

There are large uncertainties in predicting soil organic carbon (SOC) in response of future changing climate and human activities. This study estimates SOC stocks under future changing land use and climate conditions in Northeast China using a state-of-the-art digital soil mapping technique. A total of 487 soil samples and 12 environmental variables from 37 landscape units (derived from soil, topography, climate, and human activity data) combined with boosted regression trees (BRT) and random forest (RF) models are first used to map the topsoil (0–20 cm) SOC stocks in Northeast China in 2015. The primary environmental variables influencing the variability of SOC stocks are mean annual temperature, elevation, mean annual precipitation, and land use. We then applied the space-for-time substitution method in conjunction with the BRT model to predict the spatial distribution of SOC stocks under future (the 2050s and 2090s) climate and land use scenarios. SOC stocks under the scenarios of shared socioeconomic pathways (SSP245) and SSP585 (average and upper estimate of the increase in atmospheric greenhouse gases for that time) decreased by 1.5% and 4.5% in the 2050s, respectively, compared with 2015 (5293 Tg C). For the 2090s, the SOC stocks under the SSP245 scenario increased by 1.9%, and those under the SSP585 scenario decreased by 0.4%. The SOC stocks in both future periods are mainly stored in farmlands and forests, accounting for 90% and 92% of the total SOC stocks, respectively. Our high-resolution estimated SOC maps provide a scientific basis for optimizing ecological management in Northeast China.

1. Introduction

Soils contain the largest organic carbon reservoir in the biosphere and play a pivotal role in the global carbon cycle (Lal et al., 2018). Soil organic carbon (SOC) stocks are three times greater than those in the atmosphere (Riggers et al., 2021), and a slight change in soil carbon content can result in a significant amount of carbon release to the atmosphere, thereby contributing to global climate change (Lal, 2004). The concentration of greenhouse gases, such as CO₂, in the atmosphere has continued to rise and has now reached a level of 415 ppm (ppm) (Davis et al., 2010; Smith et al., 2020; Yang et al., 2022). She et al. (2022) estimated that fossil fuel CO₂ emissions in 2020 would be 34.8 Gt

Carbon (C), >50% higher than that in 1990, and reach 36.4 Gt C by 2021. Therefore, a precise evaluation of SOC stocks in terrestrial systems would help to quantify atmosphere CO₂ concentrations and their impacts on global climate.

SOC dynamics are closely linked to soil microbial activity (Post and Kwon, 2000; Bhattacharyya et al., 2022; Cui et al., 2022). Soil microbial activity plays a crucial role in modulating the decomposition rate of soil organic matter and plant litter, thereby exerting a significant impact on the SOC dynamics (McBratney et al., 2003; Ngaba et al., 2022; Mengist et al., 2023). Climate, vegetation cover, soil, and land use management all affect soil microbial activities (Albaladejo et al., 2013; Adhikari et al., 2019; Wang et al., 2022a). The rate of temperature rise has increased

* Corresponding authors at: College of Land and Environment, Shenyang Agricultural University, No. 120 Dongling Road, Shenhe District, Shenyang, Liaoning Province 110866, China.

E-mail addresses: jinxinxin0218@syou.edu.cn (X. Jin), fkqian@syou.edu.cn (F. Qian).

<https://doi.org/10.1016/j.eiar.2023.107278>

Received 13 March 2023; Received in revised form 11 August 2023; Accepted 5 September 2023

Available online 12 September 2023

0195-9255/© 2023 Elsevier Inc. All rights reserved.

significantly in the past half-century (Lal et al., 2018). With changes in the global climate and environment, terrestrial ecosystems will experience unprecedented challenges (Amelung et al., 2020). Land use change is an important driver for SOC dynamics (Meneses et al., 2017; Jiang et al., 2023). Land use changes can result in significant of greenhouse gas emissions, and the IPCC estimates that land use change and forestry activities contribute to approximately 11% of global greenhouse gas emissions (Si et al., 2021; Zhang et al., 2022). Among these land use changes, 12–17% were from land cover change (Haberl et al., 2007; Sroufe and Watts, 2022). Changes in land use patterns significantly affect SOC stocks (Fernández-Romero et al., 2014; Jiang et al., 2023). Therefore, climate and land use change are the main environmental factors that affect the spatial variability of SOC stocks (Meneses et al., 2017; Si et al., 2021; Jiang et al., 2023).

To date, extensive research on SOC stocks and its spatial distribution characteristics as well as mechanisms of SOC changes has been conducted (Martin et al., 2011; Yang et al., 2016; Jiang et al., 2023). However, the response of the SOC stocks to future climate and land use change remains uncertain (Lal, 2004; Byrd et al., 2015; Reyes Rojas et al., 2018; Adhikari et al., 2019; Wang et al., 2022b). Consequently, previous research endeavors have employed diverse global climate models and land use change scenarios to examine the impact on SOC stocks across various countries and regions (Yigini and Panagos, 2016; Reyes Rojas et al., 2018; Adhikari et al., 2019). In Wisconsin, USA, Adhikari et al. (2019) projected a potential increase of 20 Mg ha⁻¹ in SOC stocks by 2050 as a result of land use and climate change. Yigini and Panagos (2016) predicted the future SOC stock in Europe under four representative concentration pathways (RCPs), and found that the SOC stock will increase overall by 2050. Olaya-Abril et al. (2017) concluded that the SOC stocks in southern Spain may decrease by 35.4% under high emission scenarios. Although SOC stocks have been successfully predicted under future climate and land use change scenarios at both global and regional scales, an accurate and rapid tool for predicting SOC stocks is still needed. Currently, the process-based models have been used to assess the impact of climate and land use change on SOC stocks at regional and global scales, such as DNDC, RothC, CENTURY, DayCent, and CEVSA, and BIOME1.0 (Parton, 1996; Coleman and Jenkinson, 1996; Giltrap et al., 2010; Abdalla et al., 2020; Farina et al., 2021). The biggest limiting factor of these models is the need for a large amount of relevant and continuous data, increasing the difficulty of the parameterization and initialization of the model (Abdalla et al., 2020). These models often require large amounts of soil observation data, limiting their application in areas with insufficient or no soil data (Baldock et al., 2012; Abdalla et al., 2020; Smith et al., 2020).

Alternatively, McBratney et al. (2003) proposed the scorpan equation, which can be used to infer changes in SOC stocks over time. Moreover, by applying the scorpan equation, certain environmental variables can be used to predict SOC stocks. Adhikari et al. (2019) used this method to spatially predict topsoil SOC stocks in Wisconsin, USA, in 2050. This method has been widely used to predict SOC stocks under future climate and land use scenarios in the United States, Australia, Spain, Brazil, Chile, and other countries (Cerri et al., 2007; Baldock et al., 2012; Albaladejo et al., 2013; Adhikari et al., 2019; Reyes Rojas et al., 2018; Wang et al., 2022b). Notably, most studies have used multiple linear regression, polynomial regression, or stepwise regression combined with the scorpan equation to predict SOC stocks at a certain time node in the future (Byrd et al., 2015; Adhikari et al., 2019). However, such methods cannot accurately represent the continuous and gradual in soil attribute space and geographical space (McBratney et al., 2003; Smith et al., 2020). Accurate prediction of the true spatial distribution of SOC stocks is difficult using conventional methods. Recent studies show that machine learning is effective mapping SOC (Baldock et al., 2012; Adhikari et al., 2019; Wang et al., 2022a). Taken together, this study attempts to use a machine learning approach combining with the scorpan equation to predict the change in SOC stocks under future climate and land use scenarios in northeast China.

Northeast China is one of the three black soil belts worldwide and is essential for maintaining the nation's food security. Black soil has high soil organic matter, which contributes to maintaining farmland soil fertility and has an important impact on global climate change. This study aims to apply the scorpan equation to i) map the spatial distribution of topsoil (0–20 cm) SOC stocks in Northeast China in 2015, ii) determine the main environmental factors associated with SOC stocks, iii) use the equation to predict the spatiotemporal variation in SOC stocks under future climate and land use scenarios, and iv) quantify the distribution characteristics of SOC stocks under different land use patterns in the future.

2. Materials and methods

2.1. Study area

Our study area is located in Northeast China (118°–135° E, 48°–55° N), which comprise Liaoning Province, Jilin Province, and Heilongjiang Province, and spans over 0.79 million km², accounting for 8% of the national land area (Fig. 1). The gross domestic product (GDP) of this region is US\$756 billion, accounting for 5% of the national GDP of China (2020 statistics), and is inhabited by 108 million people (7.64% of the total population of China) (Wang et al., 2022a). The terrain is dominated by plains and mountains with elevations from 0 to 2665 m, where Changbai Mountain, Greater Khingan Range, and Lesser Khingan Mountain are natural barriers. The Sanjiang Plain (the easternmost), Songnen Plain (the middle), and Liaohe Plain (the southernmost) are the main agricultural areas with deep fertile soils. According to the Chinese Soil Taxonomy (Cooperative Research Group on Chinese Soil Taxonomy, 2001), the dominant soil types are Cambosols, Gleysols, and Isohumosols, which account for >80% of the total area of the region, followed by Argosols, Primosols, Anthosols, Histosols, Andosols, and Halosols. The area has a temperate monsoon climate with four distinct seasons and is warm and rainy in summer and cold and dry in winter. From the southeast to the northeast of the study area, the mean annual precipitation (MAP) decreases from 1000 mm to <300 mm and transitions from humid and semi-humid areas to semi-arid areas. The mean annual temperature (MAT) was between −4 and 11 °C. This area is important for timber and mineral production in China and is rich in wild animals and plant resources. The forest land area was approximately 0.39 × 10⁹ hm², accounting for 14.7% of the total forest area of China, and the forest coverage rate was 39.6%, far higher than the national forest coverage rate of 16.55%.

2.2. Soil samples

Because of the large spatial span, conducting intensive field surveys was impractical for soil sampling in the study area. Therefore, we applied the representativeness soil sampling method (Zhu et al. (2008)) to collect soil samples. First, the most important environmental factors affecting regional SOC stocks, such as MAT, MAP, elevation, and land use patterns, were selected, and these data were unified in a spatial coordinate system with the same spatial resolution. Second, the fuzzy c-means clustering method was used to cluster the selected environmental variables (Yang et al., 2013), and 37 clusters or landscape units were obtained. Third, local soil experts were employed to identify and locate 10–15 typical sampling points in each landscape unit, considering the accessibility and representativeness of the area. Finally, 487 soil sampling locations were identified, and the spatial information of each location was recorded using a hand-held Global Positioning System (GPSMAP 669 s, GARMIN). At each sampling location, a 1 kg mixed topsoil (0–20 cm depth) sample and 100 cm³ undisturbed soil core were collected to determine SOC and bulk density (BD). SOC was measured using a C/N analyzer (Elemental Amerivas Ins. Vario Max, Germany) by using the sampling dry burning method. Undisturbed soil cores were placed in an oven at 105 °C for 48 h to measure BD. Soil samples were

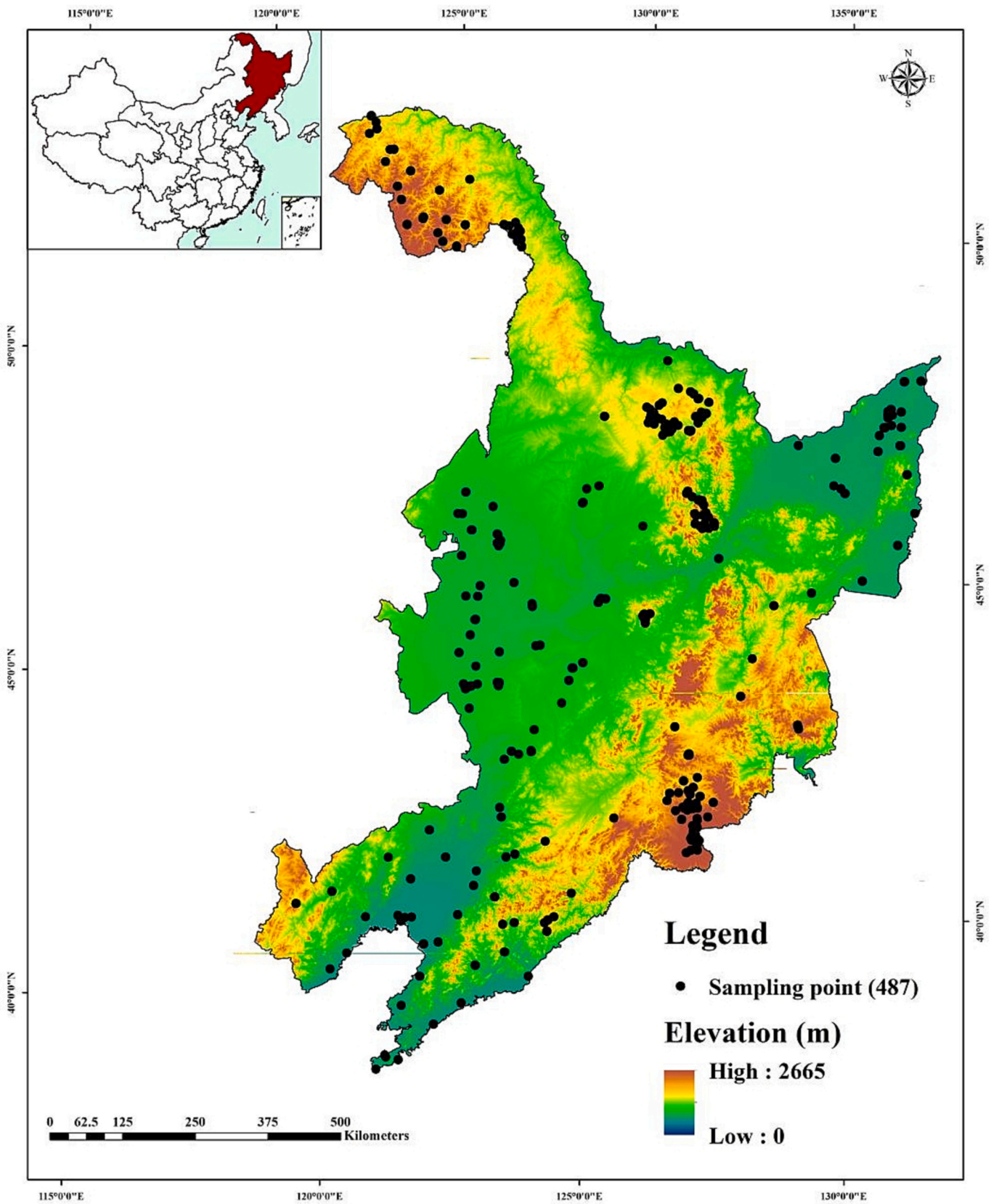


Fig. 1. Location of soil sampling points (0–20 cm) overlaid on the 90-m digital elevation model of the study area.

obtained from the Laboratory Analysis and Testing Center of Shenyang Agricultural University.

2.3. Calculation of SOC stocks

This study estimated the spatial variation in SOC stocks in different ecosystems of Northeast China under future climate and human activities. SOC stocks were calculated using Eq. 1. (Batjes, 1996):

$$SOC \text{ stocks} = SOC_{density} \times A = SOC_{content} \times BD \times D \times (1 - S) \times 10 \quad (1)$$

where $SOC_{density}$ is the SOC density ($Mg \text{ C ha}^{-1}$); A is the area of the smallest patch (ha). $SOC_{content}$ is the SOC content in mass basis ($g \text{ kg}^{-1}$); BD is the bulk density ($g \text{ cm}^{-3}$); D is the thickness (m), this study focused on the topsoil (0.2 m); S is the volume fraction of fragments $>2 \text{ mm}$ (%). In this study, all soils used were characterized by low rock content and gravel content not exceeding 2 mm. Moreover, SOC stocks at sampling points do not conform to the characteristics of Normal distribution (Table 1). Therefore, we log-transformed the SOC stock data for subsequent analysis.

2.4. Environmental variables

Twelve environmental variables from four categories (soil, topography, climate, and human activities) were used to predict the spatial distribution of SOC stocks in 2015 and the future (the 2050s and 2090s) under the SSP245 and SSP585 scenarios in different ecosystems. Because the selected environmental variables were obtained from different sources and platforms, the data were harmonized by reprojecting into a common projection system (Krasovsky_1940_Albers) and resampling to a 90 m grid resolution in ArcGIS 10.2 software (ESRI, Redlands, CA, USA) for subsequent modeling and analysis in R software (R Development Core Team, 2013).

2.4.1. Soil property data

Soil texture refers to the combination of mineral particles with different sizes and diameters in soil, which is closely related to soil aeration, fertilizer and water conservation, and the difficulty of cultivation (Galantini et al., 2004). Soil texture is an important basis for soil utilization, management, and improvement measures (Brady et al., 2008). Fertile soils have particular texture, especially for the cultivated layer (Galantini et al., 2004).

Soil texture data consisted of sand, silt, and clay percentages and were obtained from the Resource and Environment Science and Data Center of the Institute of Geographical Science and Resources, Chinese Academy of Sciences (<https://www.resdc.cn/>), at a $1 \text{ km} \times 1 \text{ km}$ resolution. The gridded data were resampled to a 90 m spatial resolution for use in this study. The data were originally compiled based on the soil

type map (1:1 million) and soil profile data obtained from the second national soil survey (1979–1985).

2.4.2. Topographic variables

Topographic variables were derived from a 90 m digital elevation model (DEM) obtained from the Geospatial Data Cloud of the Chinese Academy of Sciences (<http://www.gscloud.cn>). Six topographic variables were extracted: elevation, slope aspect (SA), slope gradient (SG), profile curvature (PC), topographic wetness index (TWI), and catchment area (CA). Elevation, SA, SG, and PC were directly calculated by ArcGIS 10.2. TWI and CA were extracted by the system for SAGA GIS software (Conrad et al., 2015).

Changes in elevation, SA, and SG influence soil-landscape processes and affect SOC distribution in a landscape (Fernández-Romero et al., 2014; Adhikari et al., 2014; Zhu et al., 2019). They also influence other environmental factors, such as water and heat flux, light interception, and soil (re)distribution (McBratney et al., 2003). TWI indicates the impact of regional topography on runoff direction and accumulation and helps identify rainfall runoff patterns, potential areas of increased soil moisture, and areas of stagnant water (Yang et al., 2016). The larger the value, the greater the soil moisture and the indirect effect on SOC stocks. CA refers to runoff area per unit contour length. CA is typically used to estimate rainfall in a small range and is one of the most commonly used variables for predicting SOC stocks (Wang et al., 2022a).

2.4.3. Climatic variables

Climatic variables comprised 1 km grid data from MAT and MAP for 2015, the 2050s, and the 2090s downloaded from the National Meteorological Information Center of the China Meteorological Administration (<http://data.cma.cn/en>). The daily precipitation and daily temperature data covering the entire northeast meteorological station in 2015 were obtained and interpolated using the inverse distance weighting algorithm. The future MAT and MAP data for the 2050s (average of 2041–2060) and 2090s (average of 2081–2100) were downloaded from the WorldClim dataset (<https://www.worldclim.org/data>). We used MAP and Map data under the Shared Socioeconomic Pathways (SSP) 245 and SSP585 paths for each period. As an update of Representative Concentration Pathway (RCP) 4.5, the additional radiation forcing of SSP245 will be 4.5 W/m^2 by 2100, which represents the middle path of future greenhouse gas emissions and assumes that climate protection measures are being implemented. SSP585 indicates that by 2100, the additional radiation forcing will be 8.5 W/m^2 , representing the upper limit of the range of situations described in the literature (Wang et al., 2022b).

2.4.4. Land use data

The change in land use type is the most intuitive manifestation of human activities, which accelerated significantly after the industrial revolution (Meneses et al., 2017). Therefore, land use data were selected

Table 1

Descriptive statistics of soil organic carbon (SOC) stocks and environmental variables were collected from sampling points in the topsoil layer (0–20 cm).

Property	Unit	Min.	Max.	Mean	SD	Skewness	Kurtosis
SOC stocks	kg m^{-2}	0.77	23.75	7.18	4.55	1.20	1.37
Elevation	m	1.00	2123.00	351.83	355.87	2.01	4.84
SG	Degree	0.00	26.39	3.28	4.66	1.98	3.58
SA	Degree	0.00	358.21	179.18	98.77	−0.04	−1.12
CA	$\text{km}^2 \text{ m}^{-1}$	0.25	190.88	220.42	20.87	3.64	21.59
TWI	Index	5.78	13.24	10.46	1.72	−0.40	−0.94
PC	Index	−0.32	0.57	0.01	0.07	1.80	18.49
MAT	mm	−7.10	10.50	2.92	3.08	−0.43	0.68
MAP	Celsius degree	426	1492	622	188	2.48	6.80
Clay	Percentage	7.00	36.00	24.35	6.87	−0.23	−0.14
Silt	Percentage	7.00	49.00	30.55	6.99	−0.72	1.48
Sand	Percentage	22.00	85.00	45.10	12.43	0.63	1.51

Note: SG, slope gradient; SA, slope aspect; CA, catchment area; TWI, topographic wetness index; PC, profile curvature; MAP, mean annual precipitation; MAT, mean annual temperature.

to reflect the impact of human activities on the soil. The land use data for 2015 were downloaded from the Resource and Environmental Science Data Center, Chinese Academy of Sciences (<https://www.resdc.cn/>), and those for the 2050s and 2090s are generated based on Geographical Simulation and Optimization System (GeoSOS) software (<http://www.geosimulation.cn>). The data from the simulated global land use data derived from the cellular automaton model based on an artificial neural network (Liu et al., 2017). The cellular automaton model is a grid dynamic model with discrete time, space, and state and local spatial interaction and temporal causality. It simulates the space-for-time evolution of complex systems (Liu et al., 2017). In addition to topographic variables, traffic maps were used to generate Euclidean distance maps in land use simulations to increase the accuracy of future land use predictions under the A1B scenario (Munoz-Rojas et al., 2013). In the A1 scenario, the world economy is assumed to continue to grow rapidly. Moreover, the world population will peak in the middle of the 21st century but will gradually decrease. The A1B scenario belongs to the A1 scenarios, characterized by a balanced mix of energy sources and resources. Assuming that climate protection measures are being implemented, A1B represents an intermediate pathway for future greenhouse gas emissions and can approximate the SSP245 path of global climate variables. In addition, because the fitting result of Liu et al. (2017) was the land use data for 2050 and 2100, we approximated the land use data for 2100 to represent the land use situation for 2090 and used it to build the model. According to China's third national land survey and land classification system, the land use types in this study were divided into farmland, forest, grassland, water, urban, and barren, and they were successively assigned the numbers 1, 2, 3, 4, 5, and 6 to facilitate model building and subsequent analysis.

2.5. Prediction models

In this study, boosted regression trees (BRT), random forest (RF), and a space-for-time substitution (STS) method were used to predict historical and future topsoil SOC stocks in Northeast China. The specific method flowchart is shown in Fig. 2.

2.5.1. Boosted regression trees

The BRT model, which can manage the nonlinear relationships between dependent and independent variables (Yang et al., 2016), was first proposed by Elith et al. (2008). A BRT combines a regression tree and boosting methods, where a regression tree is a model that combines dependent variables and their predictors with recursive binary splits. The model combines multiple simple models and improves prediction ability (Martin et al., 2011). This model can be considered as a boosting regression model, where simple trees are sequentially fitted. It encompasses various advantages based on the tree-based modeling approach (Wang et al., 2022b), including it does not require prior data conversion or outlier removal and can manage complex nonlinear relationships and interactions between predictive factors (Yang et al., 2016). The BRT model has a stronger prediction ability than traditional statistical models. The BRT model was realized by using the “dismo” and “gbm” packages in R software (R Development Core Team, 2013). The model was fine-tuned by testing different combinations of model parameters to obtain the best prediction performance. The model parameters were learning rate, tree complexity, bag fraction, and the number of trees, and their fine-tuned values were set to 0.025, 12, 0.75, and 2500, respectively.

2.5.2. Random forest

RF is a machine learning algorithm based on classification and regression trees proposed by Breiman (2001). It improves prediction accuracy without significantly increasing computational load and is insensitive to multivariate collinearity (Yang et al., 2016). The result was relatively stable despite the missing data and unbalanced data, and this model managed thousands of explanatory variables. It was known as

one of the best data mining algorithms at present (Grimm et al., 2008). The steps are as follows: 1) randomly select n subsamples from the explanatory variables, 2) establish a regression tree for each sample, 3) train and classify multiple sample data, and 4) predict (Breiman, 2001). The forest is composed of multiple regression trees. To avoid the correlation between trees, we used the bagging method to obtain different training data to increase their diversity and then extracted the dataset by replacement method. The data in the process are completely random, and a dataset can be used multiple times. The RF model was implemented in R software with the ‘randomForest’ package with model parameters $mtry$ and the NT set to 4 and 1500, respectively.

2.5.3. Space-for-time substitution method

Soil formation and development are related to climate, biology, topography, parent material, and other environmental factors (McBratney et al., 2003). The scorpan equation proposed by McBratney et al. (2003) can be used to infer the change of soil carbon storage with time. By applying the scorpan equation, we can usually to predict potential SOC stock changes in a certain period of time in the future, which is called the space-for-time (STS) substitution method (Blois et al., 2013; Gray and Bishop, 2016; Reyes Rojas et al., 2018; Adhikari et al., 2019). However, it should be noted that this method is subject to certain limitations and assumption of the stability of environmental conditions in the study area (Byrd et al., 2015; Adhikari et al., 2019). The spatial variation of SOC stocks is the result of multiple environmental factors, with climate and land use changes being identified as the primary drivers in previous studies (Davis et al., 2010; Albaladejo et al., 2013; Gray and Bishop, 2016; Reyes Rojas et al., 2018; Adhikari et al., 2019). Therefore, this study assumes that the terrain and other environmental factors will remain relatively stable over a certain period in the future, with climate and land use changes being the primary drivers of spatial variation in SOC stocks (Gray and Bishop, 2016; Reyes Rojas et al., 2018). This study employs the STS method, based on the aforementioned assumptions, to investigate alterations in SOC stocks under different climate and land use scenarios during a specific future period. However, some studies indicated that SOC stocks will not change after deforestation while soil temperature and moisture can change substantially (Nave et al., 2010; Holub and Hatten, 2019). Thus, we shall be cautious to interpret our SOC prediction results that are based on changing climate and land use conditions.

The STS method has been widely used to predict spatiotemporal changes in SOC stocks in the United States, Australia, and Brazil (Byrd et al., 2015; Smith et al., 2012; Adhikari et al., 2019; Adhikari and Hartemink, 2015). However, the lack of future SOC observations at current times and the accuracy and uncertainty of such predictions cannot be effectively verified (Gray and Bishop, 2016; Reyes Rojas et al., 2018; Adhikari et al., 2019). To predict the future (in the 2050s and 2090s) SOC stocks in the study area, we first used environmental data and SOC observations in 2015 to conduct a spatial simulation of the topsoil SOC stocks. Assuming that the terrain and parent material are relatively stable for a given period in the future, we used the STS methodology to capture potential spatiotemporal changes in SOC stocks due to changes in climate and land use.

2.6. Model validation

The accuracy of the prediction model of SOC stocks in the 2050s and 2090s depended on the prediction accuracy of the prediction model built in 2015 in the historical period. The functional relationship between SOC stocks and future environmental variables was based on a model built in 2015. To evaluate the prediction performance of the BRT and RF models in predicting SOC stocks in 2015, a 10-fold cross-validation technique combining four validation indices—mean absolute error (MAE), root mean square error (RMSE), determination of coefficient (R^2) and Lin's consistency correlation coefficient (LCCC) (Lin, 1989)—was used to compare them. The specific calculation formula is as

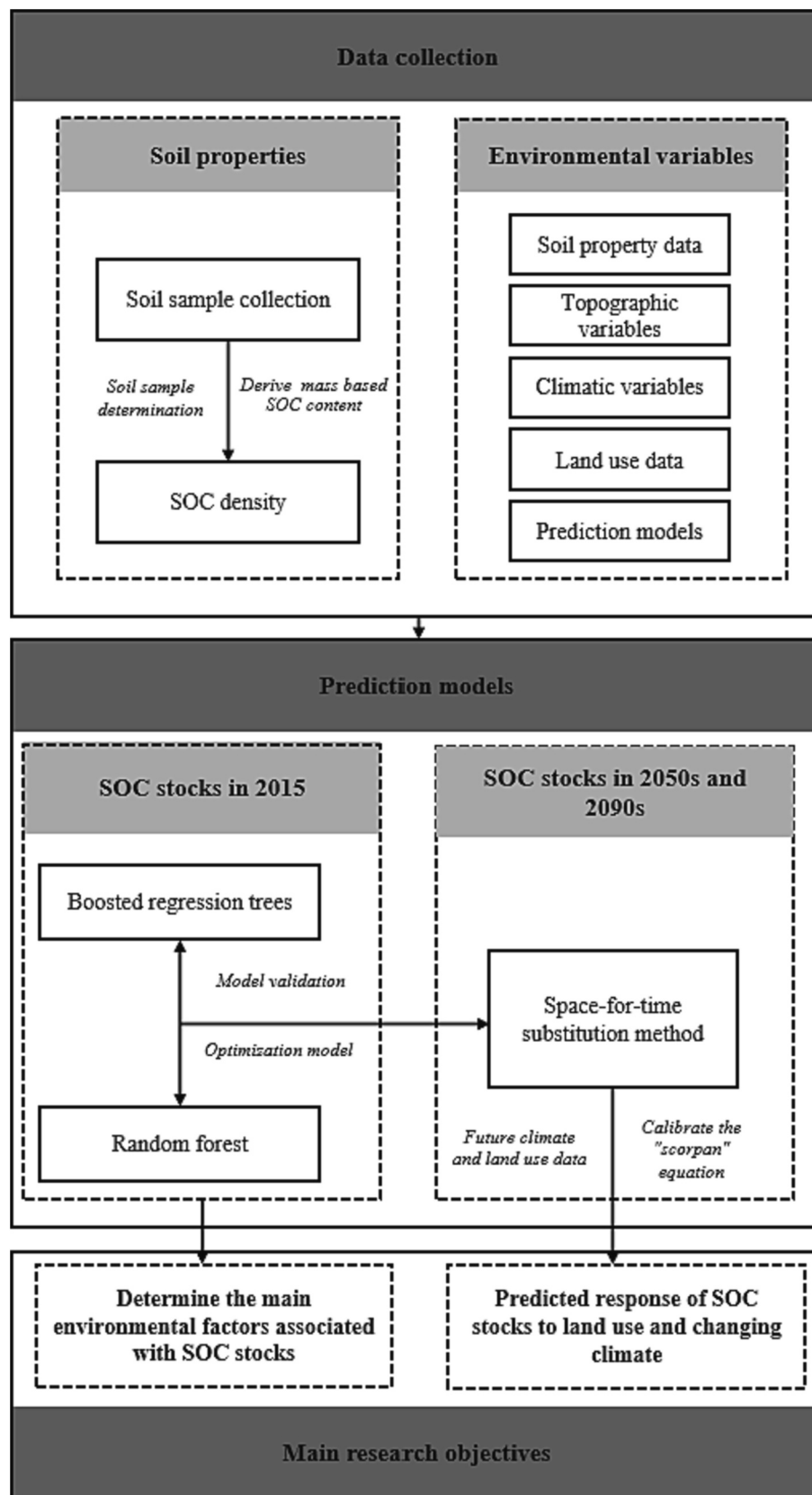


Fig. 2. Flowchart of the methodology.

follows:

$$MAE = \frac{1}{n} \sum_{i=1}^n |a_i - b_i| \tag{2}$$

$$RMSE = \sqrt{\frac{1}{n} \sum_{i=1}^n (a_i - b_i)^2} \tag{3}$$

$$R^2 = \frac{\sum_{i=1}^n (a_i - \bar{a}_i)^2}{\sum_{i=1}^n (b_i - \bar{b}_i)^2} \tag{4}$$

$$LCCC = \frac{2r\partial_a\partial_b}{\partial_a^2 + \partial_b^2 + (\bar{a} + \bar{b})^2} \tag{5}$$

where a_i , b_i , \bar{a} , \bar{b} , ∂_a , and ∂_b represent measured value, predicted value, average measured value, average predicted value, the variance of the measured set, and the variance of the predicted set, respectively, and n and r represent the number of sample points and the correlation coefficient between the predicted value and the measured value, respectively.

3. Results

3.1. Descriptive statistics

The descriptive statistics for topsoil (0–20 cm) SOC stocks and environmental variables at the 487 topsoil sampling points in 2015 are presented in Table 1. The range of topsoil SOC stocks was from 0.77 to 23.75 kg m⁻², with an average value of 7.18 kg m⁻². The skewness and kurtosis coefficients of SOC stocks were 1.2 kg m⁻² and 1.37 kg m⁻². In addition, Pearson correlation coefficients between log-transformed SOC stocks (0–20 cm) and environmental variables were calculated (Table 2). The results showed that SOC stocks were significantly and positively correlated with elevation ($r = 0.20$), SG ($r = 0.13$), LD ($r = 0.18$), MAP ($r = 0.24$), and silt ($r = 0.14$) but negatively correlated with TWI ($r = -0.17$) and MAT ($r = -0.43$). Climatic variables were significantly correlated with SOC stocks, and the correlation coefficient of MAT was -0.43 , suggesting that climatic variables played an important role in the spatial variation in regional SOC stocks.

3.2. Model performance and uncertainty

The summary statistics of 10-fold cross-validation showed that the BRT model had higher systematic R² and LCCC (0.59 and 0.73) and lower MAE and RMSE (1.99 kg m⁻² and 2.95 kg m⁻²) than the RF model (Table 3). Therefore, the BRT model was confirmed to be the best for

Table 2

Pearson correlation coefficients between log-transformed soil organic carbon (SOC) stocks and environmental variables based on 487 sampling point data in the topsoil layer (0–20 cm).

Property	SOC stocks	Elevation	SG	SA	CA	TWI	PC	LD	MAP	MAT	Clay	Silt
Elevation	0.20**											
SG	0.13**	0.47**										
SA	-0.05	0.08	0.10*									
CA	0.11*	-0.21**	-0.36**	-0.30								
TWI	-0.17**	-0.67**	-0.74**	-0.10*	0.42**							
PC	0.01	0.12**	0.16**	0.12**	-0.06	-0.12**						
LD	0.18**	-0.07	-0.10*	0.05	0.20**	0.10*	-0.03					
MAP	0.24**	0.73**	0.23**	0.09*	-0.16**	-0.41**	0.08	-0.04				
MAT	-0.43**	-0.65**	-0.21**	0.07	-0.04	0.31**	-0.08	0.07	-0.29**			
Clay	0.01	-0.01	-0.06	-0.07	-0.01	0.12*	-0.09*	-0.02	0.08			
Silt	0.14**	0.10*	-0.02	-0.05	0.09*	0.07	0.07	-0.12**	0.22**	-0.10*	0.75**	
Sand	0.02	0.07	0.13**	0.12**	-0.09*	-0.20**	-0.01	-0.20**	-0.09	0.013	-0.28**	-0.20**

Note: SG, slope gradient; SA, slope aspect; CA, catchment area; TWI, topographic wetness index; PC, profile curvature; LD, land use; MAP, mean annual precipitation; MAT, mean annual temperature.

Table 3

Summary statistics of prediction performance of boosted regression tree (BRT) and random forest (RF) models on topsoil (0–20 cm) organic carbon stocks in 2015.

Model	Index	Min.	1stQu.	Median	Mean	3rdQu.	Max.
BRT	MAE	1.93	1.98	2.00	1.99	2.02	2.04
	RMSE	2.87	2.91	2.96	2.95	2.98	3.01
	R ²	0.56	0.58	0.59	0.59	0.61	0.62
	LCCC	0.72	0.72	0.73	0.73	0.74	0.74
RF	MAE	2.12	2.13	2.15	2.15	2.16	2.18
	RMSE	2.91	2.93	2.99	3.01	3.02	3.04
	R ²	0.51	0.52	0.54	0.54	0.55	0.57
	LCCC	0.67	0.67	0.68	0.68	0.69	0.71

predicting topsoil (0–20 cm) SOC stocks in 2015. The BRT model explained approximately 59% of the spatial variability of the SOC stocks in the region (Table 3). In addition, we ran the BRT model 100 times and calculated the average of 100 iterations to represent the final predicted SOC and standard deviation (SD) as an index of prediction uncertainty (Fig. 3), and the average SD was 0.38 kg m⁻². The lower SD indicated that the BRT model had lower uncertainty and higher performance than RF model in predicting topsoil SOC stocks in Northeast China.

3.3. Relative importance of environmental factors

The BRT model was iterated 100 times, the average relative importance (RI) of 12 environmental variables was calculated, and the RI was scaled to 100%. The results showed that topographic variables (48% RI) played an important role in the spatial simulation of SOC stocks, followed by climatic variables (37%), land use data (9%), and soil property data (6%) (Fig. 4). Among the 12 environmental variables, MAT, Elevation, MAP, LD, and SG were key environmental variables, accounting for approximately 75% of the RI.

3.4. Spatial distribution of SOC stocks

The predicted topsoil (0–20 cm) SOC stocks ranged from 1.25 to 20.96 kg m⁻², with an average value of 6.72 ± 2.81 kg m⁻². The predicted maps showed that topsoil SOC stocks were higher in the north-eastern area than in the southwestern area of Northeast China. In 2015, SOC stocks were mainly stored in forests and farmland, with 2734 Tg C and 1626 Tg C, accounting for 52% and 31% of the total SOC stocks in the region, respectively (Table 5). In the 2050s, the SOC stocks under the SSP245 and SSP585 scenarios decreased by 80 Tg C and 237 Tg C, respectively, compared with 2015. In the 2090s, the SOC stocks under SSP245 and SSP585 increased by 184 Tg C and 217 Tg C, respectively, compared with the 2050s, and compared with 2015, increased by 104 Tg C (SSP245) and 19 Tg C (SSP585), respectively. SOC stocks under the

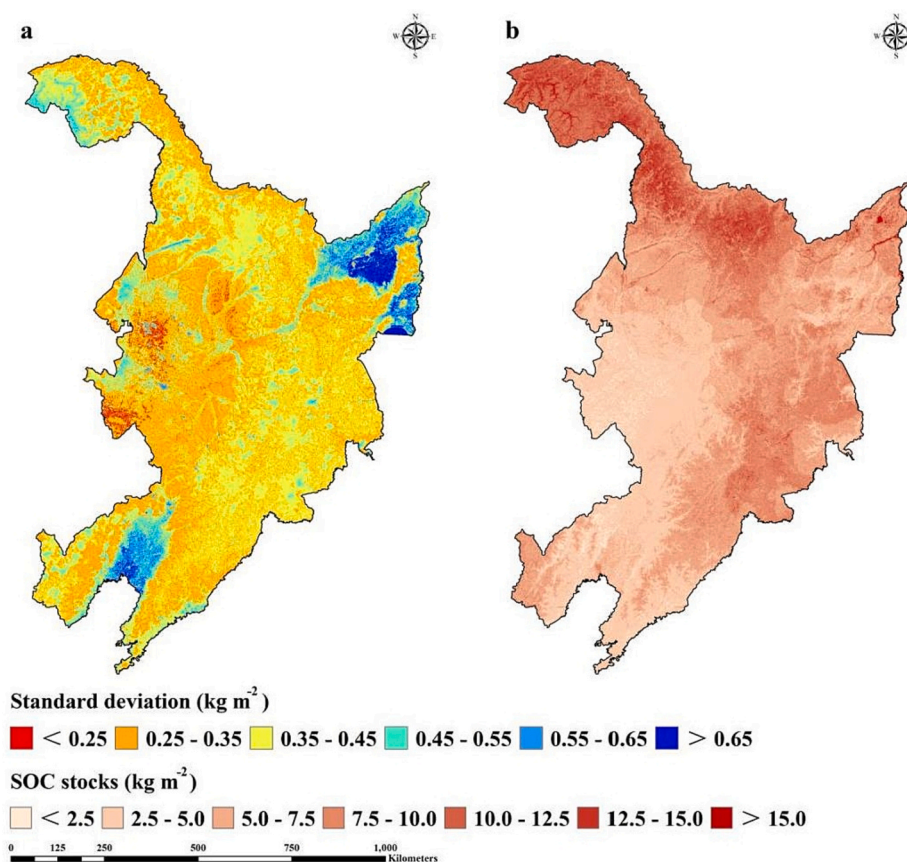


Fig. 3. Standard deviation (a) and spatial distribution (b) maps of average soil organic carbon (SOC) stock (0–20 cm) based on 100 iterations of the BRT model in 2015.

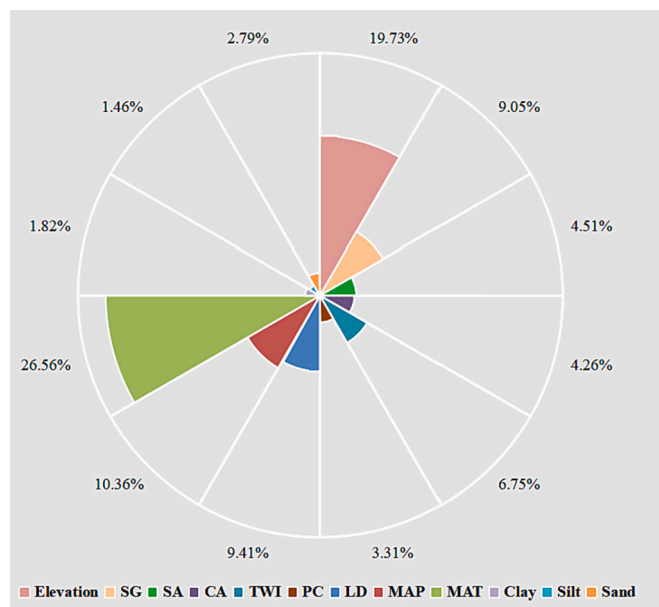


Fig. 4. Relative importance of environmental variables based on 100 iterations of the BRT model in 2015. SG, slope gradient; SA, slope aspect; CA, catchment area; TWI, topographic wetness index; PC, profile curvature; LD, land use; MAP, mean annual precipitation; MAT, mean annual temperature.

scenarios of SSP245 and SSP585 in the 2050s and 2090s had similar spatial distribution patterns (Fig. 5), with high SOC stocks distributed in the northeast and low stocks distributed in the southwest.

4. Discussion

4.1. Environmental variables and SOC stocks

In this study, soil texture, topography, climate, and land use data were selected as prediction variables for estimating historical and future SOC stocks in the topsoil of Northeast China. We observed that the distribution of SOC was significantly impacted by climatic and topographic variables. Climatic variables play a critical role in mapping the spatial distribution of SOC stocks at regional scales (Reyes Rojas et al., 2018). As reported by Yang et al. (2016), climate influences the input level of SOC through its impact on vegetation types and productivity, while also serving as the primary driver for SOC decomposition and transformation mediated by soil microorganisms (Wang et al., 2021a). Climatic variables affect microbial activity by altering soil hydrothermal conditions, thereby influencing the decomposition and transformation of SOC (Luo et al., 2017). Among climate variables, temperature and precipitation have the most significant influence on SOC stocks spatially (Wang et al., 2021b). Although it has been demonstrated that the MAP exhibits a robust correlation with SOC stocks (Reyes Rojas et al., 2018; Adhikari et al., 2019; Wang et al., 2021b; Ngaba et al., 2022), MAT was identified as the primary environmental variable governing the spatial variation of SOC stocks, accounting for 27% of RI, which has also been reported by Yang et al. (2016), Wang et al. (2021b), and Gu et al. (2022). In the humid Pampa Grassland in Argentina, Alvarez and Alvarez (2001) discovered that temperature was a more reliable predictor of SOC than precipitation. Wang et al. (2021b) investigated the temporal and spatial dynamics of topsoil SOC stocks across various ecosystems in China; revealing that MAT was a key environmental factor driving the spatial variation in SOC stocks. They further reported that colder sites exhibited higher levels of SOC stocks.

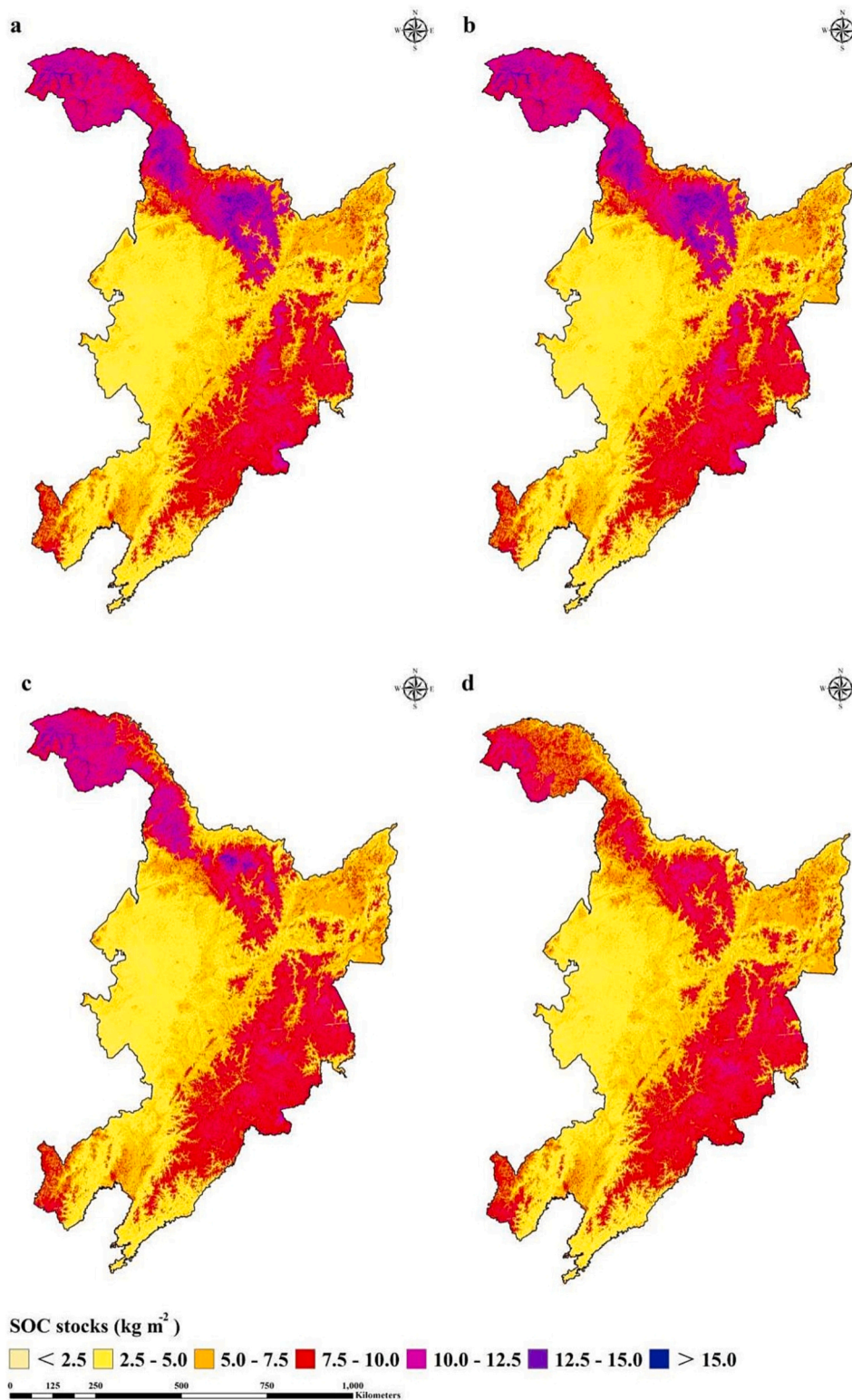


Fig. 5. Spatial distribution map of soil organic carbon (SOC) stocks (0–20 cm) under SSP245 (a: 2050s; b:2090s) and SSP585 (c: 2050s; d: 2090s) scenarios based on boosted regression tree model and the space-for-time substitution method.

Topographic variables play a crucial role in soil formation and can also impact the distribution of SOC by influencing temperature, soil moisture content, and evapotranspiration (Zhu et al., 2019). The redistribution of water and heat fluxes, which affect biomass growth, litter amount, soil microbial activities, and their biomass, are key variables that influence SOC decomposition and transformation (Fernández-

Romero et al., 2014; Yang et al., 2016; Ngaba et al., 2022). Elevation exerted the most significant influence among the topographic variables (Fig. 4), indirectly impacting SOC transformation and stocks by modulating precipitation and temperature. In Taibai Mountain, China, Zhang et al. (2020) observed a significant correlation between elevation and SOC stocks. They found SOC stocks increased with increasing elevation

at different soil depths, exhibiting an increase of 10%–88%. SG and SA are also critical for altering SOC stocks. The redistribution of water and heat conditions leads to diverse microclimates across different SA, which in turn influences the composition of vegetation community, soil formation processes, as well as plant biomass, litter amount, humification, and mineralization. Finally, the accumulation and distribution of soil carbon vary among different SA (Wang et al., 2020). SG is an important factor influencing soil erosion, and its impact on SOC primarily stems from its effect on the extent of soil erosion. Jakšić et al. (2021) concluded that SOC stocks were significantly higher on downhill and shady slopes compared to uphill and sunny slopes, respectively. TWI and CA partially reflect the soil water status in the region, with water status being a crucial factor that influences SOC mineralization. Therefore, these variables are the most frequently used topographic variables for predicting SOC stocks (Yang et al., 2016; Wang et al., 2021b; Adhikari et al., 2019).

Changes in land use or other anthropogenic activities, such as land reclamation, overgrazing, water and fertilizer utilization, and farming history also affect the spatial distribution of SOC stocks (Wang et al., 2021b, 2022a). In this study, LD was utilized as a surrogate variable for anthropogenic activities to predict SOC stocks, and the model was identified as the fourth most significant predictor (RI = 9%), following MAT, elevation, and MAP (Fig. 4). Land use change is directly correlated with topsoil coverage, disrupts the normal material cycle of the original ecosystem, alters the input source and decomposition rate of SOC, and significantly impacts underlying soil activity, SOC stock rate, and total SOC storage (Smith et al., 2012; Albaladejo et al., 2013; Adhikari et al., 2019). Changes in land use have accelerated the mineralization of SOC, leading to a rapid depletion of SOC stocks within a short period and resulting in soil degradation (Albaladejo et al., 2013).

Soil texture plays a crucial role in the distribution of SOC stock. There exists a correlation between soil texture and soil fertility, whereby soil with high clay content tend to exhibit higher levels of fertility due to their unique clay mineralogy (Galantini et al., 2004; Wang et al., 2022a; Gu et al., 2023). Galantini et al. (2004) found a positive correlation between SOC stocks and silt and clay, a negative correlation was observed with sand. In this study, with the exception of a significant positive correlation observed between silt and SOC stocks in 2015, clay and sand exhibited a negligible correlation with SOC stocks (Table 2). The land use pattern in the study area underwent substantial changes from 1990 to 2015, with farmland being converted into forest, grassland, and economic forest felling activities leading to significant alterations in soil structure (Wang et al., 2022a). Although soil texture impacts SOC dynamics, the BRT model results indicated that the RI of soil texture data was only 6%.

4.2. Predicted response of SOC stocks to land use and changing climate

According to a comparison of land use between the 2050s and 2015 in Northeast China, there will be an increase in forest and grassland areas, which can be attributed to the current government policy of returning farmland to its natural state. Farmland areas deemed

unsuitable for agriculture will be converted into forest or grassland (Li et al., 2020). Wang et al. (2021a) reported that conversion of farmland to forests would result in an annual increase in regional forest area, thereby augmenting SOC stocks. By the 2050s, under both climate scenarios (SSP245 and SSP585), approximately 90% of the total SOC stocks were predominantly stored within farmland and forests (Table 4). The primary contributing factor to this circumstance is that the study area serves as China's principal commodity grain and economic forest base, with its grain output accounting for 20% of nation's total forest area and its forest coverage representing 27% of the overall figure (Wang et al., 2022b). Additionally, the projected increase in temperatures during the 2050s is expected to enhance soil organic matter decomposition, stimulate CO₂ emissions, and reduce SOC stocks (Luo et al., 2017; Reyes Rojas et al., 2018; Adhikari et al., 2019). The anticipated increase in precipitation during the 2050s might promote plant growth and enhance SOC input; however, it may not fully offset the loss of soil carbon caused by elevated temperatures (Byrd et al., 2015). Changes in precipitation impact the availability of water to plants (Wang et al., 2022b). A decrease in precipitation can significantly diminish photosynthesis and plant growth, while an increase in precipitation can stimulate the proliferation and activity of soil microorganisms (Yang et al., 2016). However, several studies have indicated that an increase in soil moisture can mitigate the temperature sensitivity of soil respiration. Lovett (2002) suggested that the increase in precipitation and humidity played a crucial role in transforming the terrestrial ecosystem of North America into a carbon sink. Borken et al. (1999) discovered that alterations in precipitation amount or distribution can result in fluctuations of soil carbon emissions and ecosystem carbon storage. However, surprisingly, the study region's SOC stocks exhibited a declining trend in the 2050s under both climate scenarios (SSP245 and SSP585), with reductions of 80 Tg C and 236 Tg C, respectively. The topsoil exhibited the highest dynamic rate of SOC change due to fluctuations in temperature and precipitation. As explained by Rumpel et al. (2003) and Zheng et al. (2018), an increase in precipitation can result in the leaching of topsoil SOC from black land soils, which are commonly observed in our study area. Similarly, an increase in temperature and a change in precipitation pattern will accelerate the decomposition of SOC in such soils. Additionally, climate-induced intensification of soil erosion in substantial loss of soil carbon (Lal, 2002).

In the 2090s, there will be an increase in farmland and grassland areas while forest, water, urban, and barren areas will experience a decrease. The SOC stocks were projected to rise by 103 Tg C in the region under the SSP245 scenario but decline by 19 Tg C under the SSP585 scenario. In future social and economic development, it is essential to combine scientific and reasonable management of SOC with measures aimed at reducing soil carbon response to climate change. The Chinese government has been actively promoting policies that encourage the return of straw to farmland and the protection of black land (Yang et al., 2021). Each year, the government provides subsidies to farmers (Wang et al., 2021b). Furthermore, the state has invested billions of dollars in scientific research funds to study the black land in Northeast China and maintain its production capacity (Huang et al., 2019). Moreover, as a

Table 4

Summary statistics of topsoil (0–20 cm) organic carbon (SOC) stocks under different land use patterns and climate change scenarios in different periods.

Land use pattern	2015		2050s		2090s			
	Area (10 ⁴ km ²)	SOC stocks (Tg)	Area (10 ⁴ km ²)	SOC stocks (Tg)		Area (10 ⁴ km ²)	SOC stocks (Tg)	
				SSP245	SSP585		SSP245	SSP585
Farmland	30.9	1626.8	19.4	944.8	959.1	40.8	2272.7	2232.2
Forest	33.6	2734.6	47.5	3772.7	3594.1	29.3	2708.1	2630.4
Grassland	3.3	227.8	9.2	386.1	394.2	5.9	302.2	298.6
Water	1.8	100.2	0.3	20.7	20.8	0.3	20.7	20.5
Urban	3.0	155.6	1.7	88.0	87.6	1.7	88.0	87.1
Barren	5.5	448.3	0.02	0.9	0.9	0.1	5.1	5.1
Total	78.1	5293.3	78.1	5213.2	5056.7	78.1	5396.8	5273.9

result of economic development, more individuals are leaving agriculture for urban opportunities, leading to an increase in SOC stocks on abandoned lands (Liu et al., 2021; Wang et al., 2022b).

SOC stocks will exhibit diverse patterns in response to various climate scenarios in the future (Adhikari et al., 2019; Wang et al., 2022b). Our findings indicate that SOC stocks are projected to decline by 1.5% and 4.5% in the 2050s under SSP245 and SSP585 scenarios, respectively, while they are expected to increase by 1.9% under SSP245 scenario and decrease by 0.4% under SSP585 scenario in the 2090s. These findings are consistent with the results of Wang et al. (2022b), who found that SOC stocks would decline by 7.6–12.9% under SSP245 and 9.1–20.9% under SSP585 in New South Wales, Australia, by 2050. However, Adhikari et al. (2019) have demonstrated the A1B scenario would result in a 22% increase in SOC stocks by 2050 in Wisconsin, USA. Similarly, Yigini and Panagos (2016) suggested an overall increase in SOC stock across Europe by 2050 under all climate and land cover scenarios; however, the extent of this increase varied depending on the climate model and emissions scenarios. Wang et al. (2022b) posited that a declining trend is also expected to occur in the 2090s under both SSP245 and SSP585 scenarios. In southeastern Jiangsu Province, China, Song et al. (2019) demonstrated a positive trend in topsoil SOC concentration from 14.45 g kg⁻¹ in 2020 to 15.33 g kg⁻¹ in 2080, representing an increase of 7.8%. Therefore, accurate prediction of the impact of future climate change on the carbon cycle is crucial in the context of global climate change, as it provide a theoretical foundation for managing future climate change and promoting high-quality economic development.

4.3. Uncertainties in this study

Based on the higher R² and LCCC values, as well as the lower MAE and RMSE, the BRT model was selected as the final model to predict SOC stocks under different land use and climate change scenarios. Although the BRT model yielded a lower prediction error than RF model, it is important to acknowledge that there might be other sources of uncertainty associated with the prediction. For instance, in 2015, different groups analyzed the soil data which could have introduced personnel bias into the measurements. Second, environmental data were collected from various sources and GIS operations such as resampling might have introduced some errors. Third, the climatic data for both historical and future periods were sourced from disparate platforms, with no consideration given to the impact of future extreme climate events in the future or the uncertainty and inconsistency of spatial pattern across various climate factors. Fourth, the future land use data for the 2050s and 2090s were extracted from the global land use prediction database (Liu et al., 2017). However, due to limitations in data modeling methods and accuracy at that time, there may be a significant degree of uncertainty in the simulated land use data. In addition, due to the future land use dataset simulated under the A1B scenario, although both the SSP245 path under this scenario and WorldClim are simulated under the moderate development path, there are still differences that may cause bias in the final prediction results. Fifth, the soil texture data were derived from a second national soil survey conducted over 30 years ago. Nevertheless, due to significant changes in land use patterns during this period, there have been notable alterations in topsoil properties within the study area. Sixth, the prediction of SOC stocks under various future scenarios was based on historical soil environment conditions. However, it is possible that the soil environmental conditions in the future may deviate from what has been simulated. Seventh, the 497 soil samples solely assessed the topsoil at a depth of 20 cm, but there exists a greater SOC stock in the subsoil than in the topsoil, particularly within the northeast region where deep black soil is predominant. Nevertheless, the results presented in this study are based on state-of-the-art soil mapping techniques that also quantify potential model uncertainties. However, it should be noted that all relevant assumptions suggest that this may not necessarily reflect the reality we will encounter in the future, but rather represents

an intriguingly simplified version of it. We anticipate that our research findings can inform future soil management policy making in this region.

5. Conclusions

The BRT model and STS method were employed to simulate the annual and intergenerational dynamics of SOC stocks in the topsoil (0–20 cm) under future climate change conditions (the SSP245 and SSP585) and land use patterns in Northeast China for the 2050s and 2090s. In both emission scenarios, the spatial distribution was relatively similar; however, there was less loss of SOC stocks in the SSP245 scenario compared to the SSP585 scenario, and carbon accumulation was greater. The SSP585 scenario induced the decomposition of SOC, resulting in a greater loss of carbon in the source region and smaller accumulation compared to SSP245 scenario. Under the scenarios of SSP245 and SSP585, the carbon storage in the 2050s was reduced by 80 and 236 Tg C, respectively, compared to that in the historical period. In the 2090s, the SSP245 scenario exhibited a carbon sink with an increase of 101 Tg C, while the SSP585 scenario showed a carbon source. The distributions of source and sink for SOC across six land use patterns were found to be similar. These findings can assist stakeholders in managing ecosystems within the region to enhance soil carbon stocks under changing land use and climate conditions.

CRedit authorship contribution statement

Shuai Wang: Conceptualization, Investigation, Methodology, Writing – original draft. **Xingyu Zhang:** Data curation, Methodology. **Kabindra Adhikari:** Writing – review & editing. **Bol Roland:** Writing – review & editing. **Qianlai Zhuang:** Writing – review & editing. **Zicheng Wang:** Data curation, Methodology. **Di Shi:** Data curation, Methodology. **Xinxin Jin:** Funding acquisition, Investigation. **Fengkui Qian:** Writing – review & editing, Funding acquisition, Investigation.

Declaration of Competing Interest

The authors declare that they have no known competing financial interests or personal relationships that could have appeared to influence the work reported in this paper.

Data availability

The authors do not have permission to share data.

Acknowledgment

This work was funded by the National Key R&D Program of China (Grant No. 2021YFD1500200), National Natural Science Foundation of China (Grant No. 42077149), China Postdoctoral Science Foundation (Grant No. 2019 M660782), National Science and Technology Basic Resources Survey Program of China (Grant No. 2019FY101300), Scientific Research Funding Project of Liaoning Provincial (LJKMZ20220996), Doctoral research start-up fund project of Liaoning Provincial Department of Science and Technology (Grant No. 2021-BS-136), and China Scholarship Council (201908210132).

References

- Abdalla, M., Song, X., Ju, X., Topp, C.F., Smith, P., 2020. Calibration and validation of the DNDC model to estimate nitrous oxide emissions and crop productivity for a summer maize-winter wheat double cropping system in Hebei, China. *Environ. Pollut.* 262, 114199.
- Adhikari, K., Hartemink, A.E., 2015. Digital mapping of topsoil carbon content and changes in the Driftless Area of Wisconsin, USA. *Soil Sci. Soc. Am. J.* 79 (1), 155–164.

- Adhikari, K., Hartemink, A.E., Minasny, B., Bou Kheir, R., Greve, M.B., Greve, M.H., 2014. Digital mapping of soil organic carbon contents and stocks in Denmark. *PLoS One* 9 (8), e105519.
- Adhikari, K., Owens, P.R., Libohova, Z., Miller, D.M., Wills, S.A., Nemecek, J., 2019. Assessing soil organic carbon stock of Wisconsin, USA and its fate under future land use and climate change. *Sci. Total Environ.* 667, 833–845.
- Albaladejo, J., Ortiz, R., Garcia-Franco, N., Navarro, A.R., Almagro, M., Pintado, J.G., Martínez-Mena, M., 2013. Land use and climate change impacts on soil organic carbon stocks in semi-arid Spain. *J. Soils Sediments* 13 (2), 265–277.
- Alvarez, R., Alvarez, C., 2001. Temperature regulation of soil carbon dioxide production in the humid Pampa of Argentina: estimation of carbon fluxes under climate change. *Biol. Fertil. Soils* 34 (4), 282–285.
- Amelung, W., Bossio, D., de Vries, W., Kögel-Knabner, I., Lehmann, J., Amundson, R., Chabbi, A., 2020. Towards a global-scale soil climate mitigation strategy. *Nat. Commun.* 11 (1), 1–10.
- Baldock, J.A., Wheeler, I., McKenzie, N., McBratney, A., 2012. Soils and climate change: potential impacts on carbon stocks and greenhouse gas emissions, and future research for Australian agriculture. *Crop Pasture Sci.* 63 (3), 269–283.
- Batjes, N.H., 1996. Total carbon and nitrogen in the soils of the world. *Eur. J. Soil Sci.* 47 (2), 151–163.
- Bhattacharyya, S.S., Ros, G.H., Furtak, K., Iqbal, H.M., Parra-Saldívar, R., 2022. Soil carbon sequestration—an interplay between soil microbial community and soil organic matter dynamics. *Sci. Total Environ.* 152928.
- Blois, J.L., Williams, J.W., Fitzpatrick, M.C., Jackson, S.T., Ferrier, S., 2013. Space can substitute for time in predicting climate-change effects on biodiversity. *Proc. Natl. Acad. Sci.* 110 (23), 9374–9379.
- Borken, W., Xu, Y.J., Brumme, R., Lamersdorf, N., 1999. A climate change scenario for carbon dioxide and dissolved organic carbon fluxes from a temperate forest soil drought and rewetting effects. *Soil Sci. Soc. Am. J.* 63 (6), 1848–1855.
- Brady, N.C., Weil, R.R., 2008. *The Nature and Properties of Soils*, vol. 13. Prentice Hall, Upper Saddle River, NJ, pp. 662–710.
- Breiman, L., 2001. Random forests. *Mach. Learn.* 45 (1), 5–32.
- Byrd, K.B., Flint, L.E., Alvarez, P., Casey, C.F., Sleeter, B.M., Soular, C.E., Sohl, T.L., 2015. Integrated climate and land use change scenarios for California rangeland ecosystem services: wildlife habitat, soil carbon, and water supply. *Landsc. Ecol.* 30 (4), 729–750.
- Cerri, C.E.P., Easter, M., Paustian, K., Killian, K., Coleman, K., Bernoux, M., Cerri, C.C., 2007. Predicted soil organic carbon stocks and changes in the Brazilian Amazon between 2000 and 2030. *Agric. Ecosyst. Environ.* 122 (1), 58–72.
- Coleman, K., Jenkinson, D.S., 1996. RothC-26.3-a model for the turnover of carbon in soil. In: *Evaluation of Soil Organic Matter Models*. Springer, Berlin, Heidelberg, pp. 237–246.
- Conrad, O., Bechtel, B., Bock, M., Dietrich, H., Fischer, E., Gerlitz, L., Wehberg, J., Wichmann, V., Boehner, J., 2015. System for Automated Geoscientific Analyses (SAGA) v. 2.1.4. *Geosci. Model Dev.* 8, 1991–2007.
- Cooperative Research Group on Chinese Soil Taxonomy, 2001. *Keys to Chinese Soil Taxonomy*. Press of University of Science and Technology of China, Hefei, China (in Chinese).
- Cui, Y., Khan, S.U., Deng, Y., Zhao, M., 2022. Spatiotemporal heterogeneity, convergence and its impact factors: perspective of carbon emission intensity and carbon emission per capita considering carbon sink effect. *Environ. Impact Assess. Rev.* 92, 106699.
- Davis, S.J., Caldeira, K., Matthews, H.D., 2010. Future CO₂ emissions and climate change from existing energy infrastructure. *Science* 329 (5997), 1330–1333.
- Elith, J., Leathwick, J.R., Hastie, T., 2008. A working guide to boosted regression trees. *J. Anim. Ecol.* 77 (4), 802–813.
- Farina, R., Sándor, R., Abdalla, M., Álvaro-Fuentes, J., Bechini, L., Bolinder, M.A., Bellocchi, G., 2021. Ensemble modelling, uncertainty and robust predictions of organic carbon in long-term bare-fallow soils. *Glob. Chang. Biol.* 27 (4), 904–928.
- Fernández-Romero, M.L., Lozano-García, B., Parras-Alcántara, L., 2014. Topography and land use change effects on the soil organic carbon stock of forest soils in Mediterranean natural areas. *Agric. Ecosyst. Environ.* 195, 1–9.
- Galantini, J.A., Senesi, N., Brunetti, G., Rosell, R., 2004. Influence of texture on organic matter distribution and quality and nitrogen and sulphur status in semiarid Pampean grassland soils of Argentina. *Geoderma*, 123(1–2), 143–152.
- Giltrap, D.L., Li, C., Saggat, S., 2010. DNDC: a process-based model of greenhouse gas fluxes from agricultural soils. *Agric. Ecosyst. Environ.* 136 (3–4), 292–300.
- Gray, J.M., Bishop, T.F., 2016. Change in soil organic carbon stocks under 12 climate change projections over New South Wales, Australia. *Soil Sci. Soc. Am. J.* 80 (5), 1296–1307.
- Grimm, R., Behrens, T., Märker, M., Elsenbeer, H., 2008. Soil organic carbon concentrations and stocks on Barro Colorado Island—digital soil mapping using random forests analysis. *Geoderma*, 146(1–2), 102–113.
- Gu, J., Bol, R., Sun, Y., Zhang, H., 2022. Soil carbon quantity and form are controlled predominantly by mean annual temperature along 4000 km North-South transect of Eastern China. *Catena* 217, 106498.
- Gu, J., Bol, R., Wang, Y., Zhang, H., 2023. Controls on soil dissolved organic carbon along the 4000 km North-South forest transect in Eastern China. *Catena* 220, 106691.
- Haberl, H., Erb, K.H., Krausmann, F., Gaube, V., Bondeau, A., Plutzer, C., Fischer-Kowalski, M., 2007. Quantifying and mapping the human appropriation of net primary production in earth's terrestrial ecosystems. *Proc. Natl. Acad. Sci.* 104 (31), 12942–12947.
- Holub, S.M., Hatten, J.A., 2019. Soil carbon storage in Douglas-fir forests of western Oregon and Washington before and after modern timber harvesting practices. *Soil Sci. Soc. Am. J.* 83 (s1), S175–S186.
- Huang, D., Du, P., Walling, D.E., Ning, D., Wei, X., Liu, B., Wang, J., 2019. Using reservoir deposits to reconstruct the impact of recent changes in land management on sediment yield and sediment sources for a small catchment in the Black Soil region of Northeast China. *Geoderma* 343, 139–154.
- Jakšić, S., Ninkov, J., Milić, S., Vasin, J., Živanov, M., Jakšić, D., Komlen, V., 2021. Influence of slope gradient and aspect on soil organic carbon content in the region of Niš, Serbia. *Sustainability* 13 (15), 8332.
- Jiang, W., Li, Z., Xie, H., Ouyang, K., Yuan, H., Duan, L., 2023. Land use change impacts on red slate soil aggregates and associated organic carbon in diverse soil layers in subtropical China. *Sci. Total Environ.* 856, 159194.
- Lal, R., 2002. Soil carbon sequestration in China through agricultural intensification, and restoration of degraded and desertified ecosystems. *Land Degrad. Dev.* 13 (6), 469–478.
- Lal, R., 2004. Soil carbon sequestration impacts on global climate change and food security. *science* 304 (5677), 1623–1627.
- Lal, R., Kimble, J., Follett, R.F., 2018. *Pedospheric processes and the carbon cycle. In: Soil Processes and the Carbon Cycle*. CRC press, pp. 1–8.
- Li, Z., Sun, X., Huang, Z., Zhang, X., Wang, Z., Li, S., Zhai, B., 2020. Changes in nutrient balance, environmental effects, and green development after returning farmland to forests: a case study in Ningxia, China. *Sci. Total Environ.* 735, 139370.
- Lin, L., 1989. A concordance correlation coefficient to evaluate reproducibility. *Biometrics* 45, 255–268.
- Liu, X., Liang, X., Li, X., Xu, X., Ou, J., Chen, Y., Pei, F., 2017. A future land use simulation model (FLUS) for simulating multiple land use scenarios by coupling human and natural effects. *Landsc. Urban Plan.* 168, 94–116.
- Liu, G., Bai, Z., Shah, F., Cui, G., Xiao, Z., Gong, H., Shah, S., 2021. Compositional and structural changes in soil microbial communities in response to straw mulching and plant revegetation in an abandoned artificial pasture in Northeast China. *Glob. Ecol. Conserv.* 31, e01871.
- Lovett, R.A., 2002. Rain might be leading carbon sink factor. *Science* 1787.
- Luo, Z., Feng, W., Luo, Y., Baldock, J., Wang, E., 2017. Soil organic carbon dynamics jointly controlled by climate, carbon inputs, soil properties and soil carbon fractions. *Glob. Chang. Biol.* 23 (10), 4430–4439.
- Martin, M.P., Wattenbach, M., Smith, P., Meersmans, J., Jolivet, C., Boulonne, L., Arrouays, D., 2011. Spatial distribution of soil organic carbon stocks in France. *Biogeosciences* 8 (5), 1053–1065.
- McBratney, A.B., Santos, M.M., Minasny, B., 2003. On digital soil mapping. *Geoderma* 117 (1–2), 3–52.
- Meneses, B.M., Reis, E., Pereira, S., Vale, M.J., Reis, R., 2017. Understanding driving forces and implications associated with the land use and land cover changes in Portugal. *Sustainability* 9 (3), 351.
- Mengist, W., Soromessa, T., Feyisa, G.L., 2023. Responses of carbon sequestration service for landscape dynamics in the Kaffa biosphere reserve, Southwest Ethiopia. *Environ. Impact Assess. Rev.* 98, 106960.
- Munoz-Rojas, M., Jordán, A., Zavala, L.M., González-Peñalosa, F.A., De la Rosa, D., Pino-Mejías, R., Anaya-Romero, M., 2013. Modelling soil organic carbon stocks in global change scenarios: a CarboSOIL application. *Biogeosciences* 10 (12), 8253–8268.
- Nave, L.E., Vance, E.D., Swanston, C.W., et al., 2010. Harvest impacts on soil carbon storage in temperate forests. *For. Ecol. Manag.* 259 (5), 857–866.
- Ngaba, M.J.Y., Uwiragiye, Y., Bol, R., de Vries, W., Jian, J., Zhou, J., 2022. Global cross-biome patterns of soil respiration responses to individual and interactive effects of nitrogen addition, altered precipitation, and warming. *Sci. Total Environ.* 159808.
- Olaya-Abril, Alfonso, Parras-Alcantara, Luis, Lozano-García, Beatriz, Obregón-Romero, Rafael, 2017. Soil organic carbon distribution in Mediterranean areas under a climate change scenario via multiple linear regression analysis. *Sci. Total Environ.* 592, 134–143.
- Parton, W.J., 1996. The CENTURY model. In: *Evaluation of Soil Organic Matter Models*. Springer, Berlin, Heidelberg, pp. 283–291.
- Post, W.M., Kwon, K.C., 2000. Soil carbon sequestration and land-use change: processes and potential. *Glob. Chang. Biol.* 6 (3), 317–327.
- R Development Core Team, 2013. *R: A Language and Environment for Statistical Computing*. R Foundation for Statistical Computing, Vienna, Austria. <https://www.r-project.org/>.
- Reyes Rojas, L.A., Adhikari, K., Ventura, S.J., 2018. Projecting soil organic carbon distribution in Central Chile under future climate scenarios. *J. Environ. Qual.* 47 (4), 735–745.
- Riggers, C., Poeplau, C., Don, A., Frühauf, C., Dechow, R., 2021. How much carbon input is required to preserve or increase projected soil organic carbon stocks in German croplands under climate change? *Plant Soil* 460 (1), 417–433.
- Rumpel, C., Balesdent, J., Grootes, P., Weber, E., Kögel-Knabner, I., 2003. Quantification of lignite-and vegetation-derived soil carbon using 14C activity measurements in a forested chronosequence. *Geoderma* 112 (1–2), 155–166.
- She, X., Wang, Y., Xu, H., Tsang, S.C.E., Lau, S.P., 2022. Challenges and opportunities of electrocatalytic CO₂ reduction to chemicals and fuels. *Angew. Chem. Int. Ed.* 61 (49), 202211396.
- Si, R., Aziz, N., Raza, A., 2021. Short and long-run causal effects of agriculture, forestry, and other land use on greenhouse gas emissions: evidence from China using VECM approach. *Environ. Sci. Pollut. R.* 28 (45), 64419–64430.
- Smith, P., Davies, C.A., Ogle, S., Zanchi, G., Bellarby, J., Bird, N., Braimoh, A.K., 2012. Towards an integrated global framework to assess the impacts of land use and management change on soil carbon: current capability and future vision. *Glob. Chang. Biol.* 18 (7), 2089–2101.
- Smith, P., Soussana, J.F., Angers, D., Schipper, L., Chenu, C., Rasse, D.P., Klumpp, K., 2020. How to measure, report and verify soil carbon change to realize the potential of soil carbon sequestration for atmospheric greenhouse gas removal. *Glob. Chang. Biol.* 26 (1), 219–241.

- Song, X.D., Yang, J.Y., Zhao, M.S., Zhang, G.L., Liu, F., Wu, H.Y., 2019. Heuristic cellular automaton model for simulating soil organic carbon under land use and climate change: a case study in eastern China. *Agric. Ecosyst. Environ.* 269, 156–166.
- Sroufe, R., Watts, A., 2022. Pathways to agricultural DECARBONIZATION: climate change obstacles and opportunities in the US. *Resour. Conserv. Recycl.* 182, 106276.
- Wang, S., Adhikari, K., Zhuang, Q., Gu, H., Jin, X., 2020. Impacts of urbanization on soil organic carbon stocks in the northeast coastal agricultural areas of China. *Sci. Total Environ.* 721, 137814.
- Wang, Q., Cao, X., Wang, C., Li, H., He, J., Lu, C., 2021a. Research progress of no/minimum tillage corn seeding technology and machine in northeast black land of China. *Nongye Jixie Xuebao/Transactions of the Chinese Society of Agricultural Machinery* 52 (10).
- Wang, S., Xu, L., Zhuang, Q., He, N., 2021b. Investigating the spatio-temporal variability of soil organic carbon stocks in different ecosystems of China. *Sci. Total Environ.* 758, 143644.
- Wang, B., Gray, J.M., Waters, C.M., Anwar, M.R., Orgill, S.E., Cowie, A.L., Li Liu, D., 2022a. Modelling and mapping soil organic carbon stocks under future climate change in South-Eastern Australia. *Geoderma* 405, 115442.
- Wang, S., Zhou, M., Adhikari, K., Zhuang, Q., Bian, Z., Wang, Y., Jin, X., 2022b. Anthropogenic controls over soil organic carbon distribution from the cultivated lands in Northeast China. *Catena* 210, 105897.
- Yang, L., Zhu, A.X., Qi, F., Qin, C.Z., Li, B.L., T. P., 2013. An integrative hierarchical stepwise sampling strategy and its application in digital soil mapping. *Int. J. Geogr. Inf. Sci.* 27 (1), 1–23.
- Yang, R., Zhang, G., Liu, F., Lu, Y., Yang, F., Yang, F., Yang, M., Zhao, Y., Li, D., 2016. Comparison of boosted regression tree and random forest models for mapping topsoil organic carbon concentration in an alpine ecosystem. *Ecol. Indic.* 60, 870–878.
- Yang, W., Li, S., Wang, X., Liu, F., Li, X., Zhu, X., 2021. Soil properties and geography shape arbuscular mycorrhizal fungal communities in black land of China. *Appl. Soil Ecol.* 167, 104109.
- Yang, M., Hou, Y., Wang, Q., 2022. Rethinking on regional CO₂ allocation in China: a consideration of the carbon sink. *Environ. Impact Assess. Rev.* 96, 106822.
- Yigini, Y., Panagos, P., 2016. Assessment of soil organic carbon stocks under future climate and land cover changes in Europe. *Sci. Total Environ.* 557, 838–850.
- Zhang, Y.J., Yu, Y.C., Niu, J.J., Gong, L.L., 2020. The elevational patterns of soil organic carbon storage on the northern slope of Taibai Mountain of Qinling. *Acta Ecol. Sinica* 40 (2), 629–639.
- Zhang, Y., Meng, W., Yun, H., Xu, W., Hu, B., He, M., Zhang, L., 2022. Is urban green space a carbon sink or source?—a case study of China based on LCA method. *Environ. Impact Assess. Rev.* 94, 106766.
- Zheng, H., Liu, W., Zheng, J., Luo, Y., Li, R., Wang, H., Qi, H., 2018. Effect of long-term tillage on soil aggregates and aggregate-associated carbon in black soil of Northeast China. *PLoS One* 13 (6), e0199523.
- Zhu, A.X., Yang, L., Li, B., Qin, C., English, E., Burt, J.E., Zhou, C., 2008. Purposive sampling for digital soil mapping for areas with limited data. In: Hartemink, A.E. (Ed.), *Digital Soil Mapping with Limited Data*. Springer, pp. 33–245.
- Zhu, M., Feng, Q., Qin, Y., Cao, J., Zhang, M., Liu, W., Li, B., 2019. The role of topography in shaping the spatial patterns of soil organic carbon. *Catena* 176, 296–305.